Analysis of additional array performance metrics

1. SLL control

With respect to the sidelobe level (SLL) control, as formulated in problem (9), it should be clarified that the objective of the proposed algorithm is to constrain the SLL no higher than a prescribed threshold ρ, not to minimize it. To further demonstrate the SLL control capability of the proposed algorithm in an explicit way, we summarize the SLL values of the power gain patterns obtained by different algorithms (from Fig. 4 and Fig. 6) in tables below:

Table. R1: The SLL obtained by all algorithms in Fig. 4

	SBPS_{11}	SBPS_{12}	SBPS_{21}	SBPS_{22}	PGPS [23]	**Proposed**
$G_{\min} = 10\mathrm{dBi}$	-12.0 dB	-44.9 dB	-12.0 dB	-43.7 dB	-12.0 dB	**-15.9 dB**
$G_{\min} = 8\mathrm{dBi}$	-12.0 dB	-50.8 dB	-12.0 dB	-45.4 dB	-12.0 dB	**-17.6 dB**
$G_{\min} = 6\mathrm{dBi}$	-12.0 dB	-54.9 dB	-12.0 dB	-38.0 dB	-12.0 dB	**-17.8 dB**
$G_{\min} = 4\mathrm{dBi}$	-12.0 dB	-54.1 dB	-12.0 dB	-38.9 dB	-12.0 dB	**-13.2 dB**

Table. R2: The SLL obtained by all algorithms in Fig. 6

	SBPS_{11}	SBPS_{12}	SBPS_{21}	SBPS_{22}	PGPS [23]	**Proposed**
$G_{\min} = 10\mathrm{dBi}$	-12.0 dB	-52.1 dB	-12.0 dB	-47.9 dB	-12.0 dB	**-19.5 dB**
$G_{\min} = 8\mathrm{dBi}$	-12.0 dB	-48.0 dB	-12.0 dB	-46.5 dB	-12.0 dB	**-20.3 dB**
$G_{\min} = 6\mathrm{dBi}$	-12.0 dB	-46.7 dB	-12.0 dB	-45.2 dB	-12.0 dB	**-18.6 dB**
$G_{\min} = 4\mathrm{dBi}$	-12.0 dB	-62.1 dB	-12.0 dB	-44.8 dB	-12.0 dB	**-17.1 dB**

The desired SLL is uniformly set to -12 dB (i.e., $\rho = 10^{(-12/10)}$) for all compared SBPS_{11} , SBPS_{21} , the existing PGPS-based algorithm in [23] and the proposed algorithm, which can explicitly constrain the SLL. As presented in Table. R1 and Table. R2, the SLL obtained by these algorithms consistently maintains no higher than this threshold in all scenarios. In addition, since the optimization objective of SBPS_{12} and SBPS_{22} is to minimize the SLL, both of them can obtain a relatively low SLL. Hence, the effectiveness of the proposed algorithm in enforcing the prescribed SLL constraint is validated.

2. Scanning capability

Since the objective of this Communication is widening the array mainlobe beamwidth (AMB), the scanning performance is evaluated under scenarios where the mainlobe is steered toward different directions.

We compare the AMB obtained by the proposed algorithm with other existing algorithms given different mainlobe centering directions θ_c, i.e., $\theta_c =$ 80°, 70°, 60°. The parameter settings are the same as those for Fig. 4, with $G_{\min} = 4\text{dBi}$ (the desired minimum mainlobe power gain) in all scenarios. The resulting figures and data are provided below:

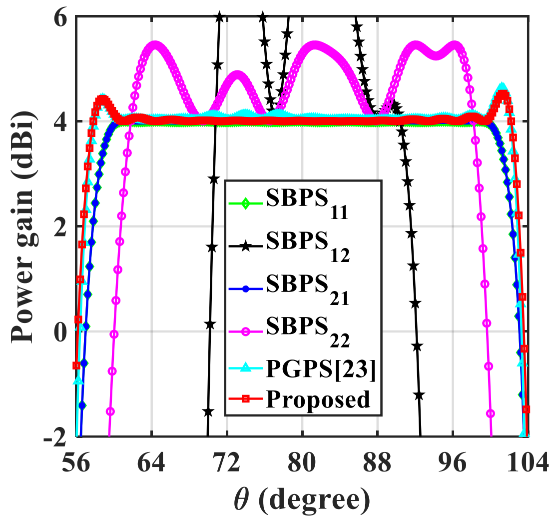

Fig. R1(a): Power gain patterns synthesized by different algorithms with θ_c = 80°.

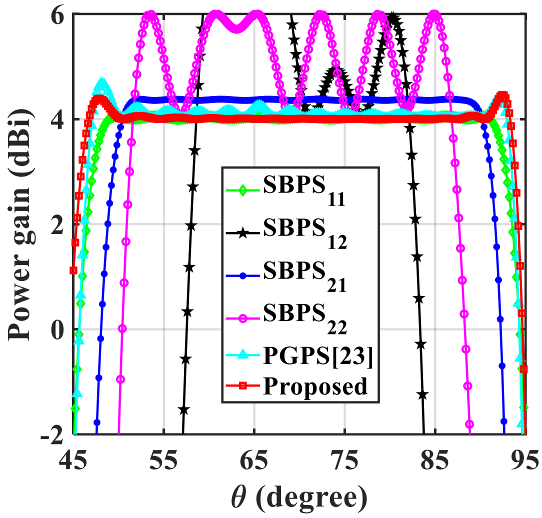

Fig. R1(b): Power gain patterns synthesized by different algorithms with $\theta_c = 70°$.

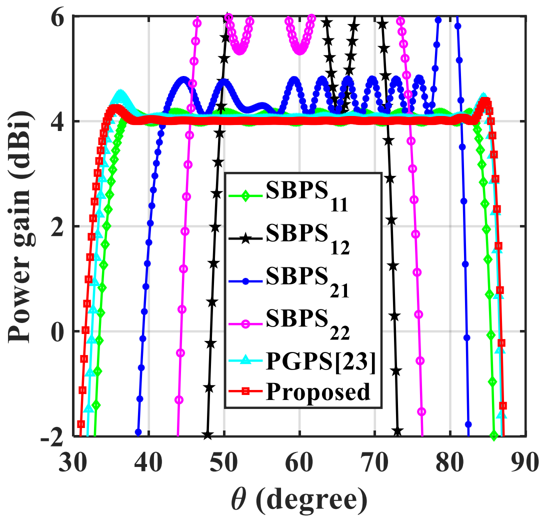

Fig. R1(c) Power gain patterns synthesized by different algorithms with $\theta_c = 60°$.

Table.R3: The AMB obtained by all algorithms given different θ_c with $G_{\min} = 4\text{dBi}$

	$SBPS_{11}$	$SBPS_{12}$	$SBPS_{21}$	$SBPS_{22}$	PGPS [23]	**Proposed**
$\theta_c = 80°$	38.8°	20.6°	38.8°	36.4°	44.2°	**44.4°**
$\theta_c = 70°$	42.0°	24.2°	40.2°	33.6°	45.8°	**46.6°**
$\theta_c = 60°$	46.6°	23.2°	42.8°	29.2°	50.4°	**50.8°**

Notably, the performance of all algorithms varies with different mainlobe center angles θ_c. However, the proposed algorithm consistently achieves the widest AMB across all scenarios, as shown in Table. R3. From Fig. R1, it can be observed that as θ_c gradually deviates from the original 90°, significant performance fluctuations and ripples emerge in the power gain patterns of three out of the four SBPS-based methods (i.e., SBPS_{12}, SBPS_{21}, SBPS_{22}), while SBPS_{11} remains relatively stable. In contrast, both PGPS-based approaches (i.e., the existing PGPS-based algorithm from [23] and the proposed algorithm), demonstrate competitive robustness.

3. Scalability with respect to array sizes

We have extended simulations to different array size, where the number of antenna elements is denoted by *N*. Specifically, the simulations involve sizes of $N = 21$, 81, 121 and 201, covering both small and medium-scale scenarios.

All the simulations are performed on a uniformly distributed array with $G_{\min} = 4\mathrm{dBi}$. The corresponding results of different algorithms are presented as follows:

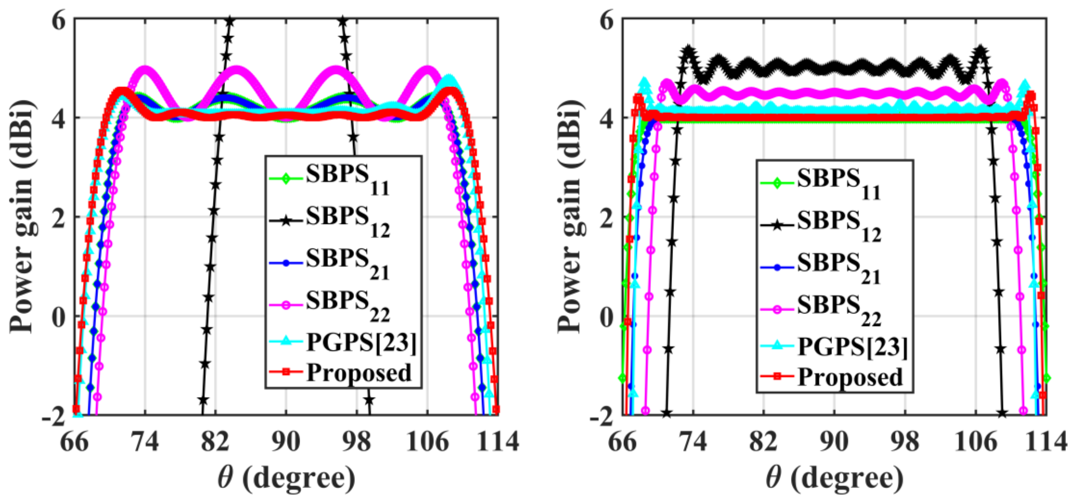

(a) $N = 21$ (b) $N = 81$

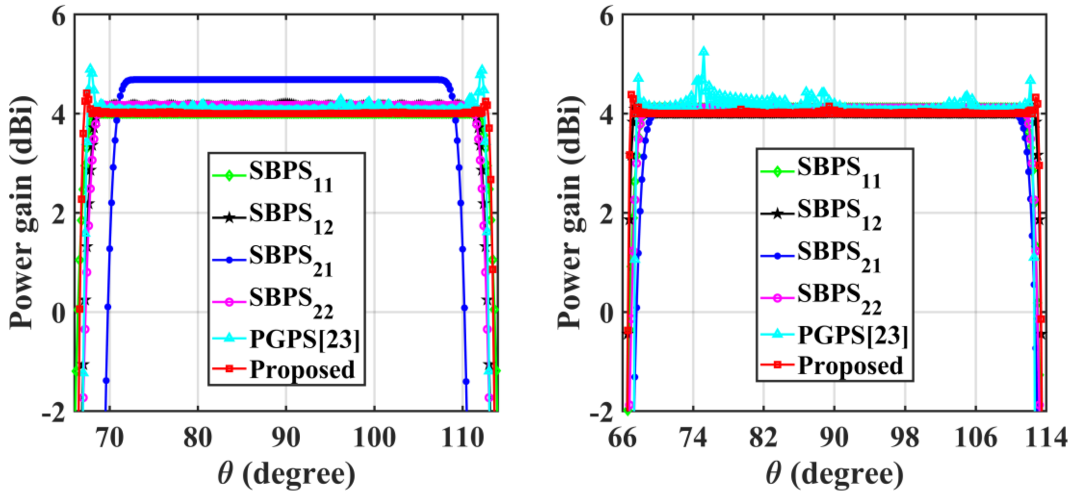

(c) $N = 121$ (d) $N = 201$

Fig. R2: Power gain patterns synthesized via the uniformly distributed array with different array sizes when $G_{\min} = 4\text{dBi}$.

Table. R4: The AMB obtained by all algorithms via the uniformly distributed array with different array sizes when $G_{\min} = 4\text{dBi}$.

	$SBPS_{11}$	$SBPS_{12}$	$SBPS_{21}$	$SBPS_{22}$	PGPS [23]	**Proposed**
N = 21	37.2°	14.8°	37.2°	36.8°	40.4°	**40.8°**
N = 81	40.6°	35.4°	39.2°	39.8°	44.0°	**45.2°**
N = 121	42.6°	43.0°	38.2°	42.6°	45.0°	**45.8°**
N = 201	43.0°	45.2°	40.8°	43.4°	44.8°	**46.0°**

Based on Fig. R2 and Table R4, it is clear that the proposed algorithm demonstrates robust and competitive performance, as it consistently achieves the widest AMB compared to other algorithms across all array sizes, which validates its scalability.

Regarding the large-scale scenario ($N > 1000$), we would like to clarify that our proposed method and those comparing methods are based on iterative convex optimization via the CVX toolbox. It is known that the computational complexity of solving semidefinite programming (SDP) or second-order cone programming (SOCP) problems scales non-linearly with the number of variables. Hence, simulating arrays with $N > 1000$ is computationally prohibitive for iterative convex optimization solvers.

Consequently, we conduct our simulations over the range $N = 21$ to 201. At the current stage, synthesizing large-scale arrays (e.g., with more than 1000 elements) via iterative convex optimization remains challenging, which represents a promising research topic for the antenna and propagation community.